EXPERIMENTAL STUDY ON EFFECT OF STONE ARCH BRIDGE ON FLOOD FLOW AND ITS STABILITY AGAINST FLOOD PRESSURE

By Yasunori KONISHI*

The region of Nagasaki, Kyushu, Japan was inundated by heavy rainfall on the 23 rd of July, 1982, and water flow of the River Nakajima and other rivers increased remarkably in this area. Many rivers in Kyushu are spanned by stone arch bridges.

To study on the effect of flood flow on a stone arch bridge and to measure fluid pressure that may damage the bridge, a solid model of Fukuro bridge and a model stone masonry arch were prepared in the experimental water channel at Nagasaki University.

The experiment was performed for two cases : in the first case the model stone arch was set in the water channel and in the second case no model arch was used. For each case, the hydraulic data and the resultant drag and down-pull forces working on the arch stones, were measured. Using the external forces obtained in the both tests, the stability of the stone arch bridge was calculated for the flood flow. The calculation confirmed that the arch stones of the Fukuro bridge could withstand the flood.

Keywords : stone arch bridge, flood flow, stability against flood pressure

1. OUTLINE

A heavy local downpour hit the Nagasaki area of Kyushu Island on July 23, 1982, causing a sudden increase of water flow in many rivers so that the flow reached the superstructures of bridges on the Uragami, Nakajima, Hachiro and other rivers. The flow spped was also fast; for example in the main stream of the River Uragami running in front of Matsuyama Stadium, it was 3.5 meters per second.

In Kyushu, including Nagasaki, Kumamoto and Kagosima prefectures, there still remain many rivers spanned by stone arch bridges. The stone arch bridges were constructed by a traditional method which was one of the most reliable methods of bridge construction, as well proven by many ancient Roman Bridges still stoutly remaining after some two thousand years and attracting tourists for their beauty. The oldest existing stone bridge in Japan is the Megane Bridge constructed in 1634 across the River Nakajima in Nagasaki City. While such stone bridges are a valuable property in the history of building techniques, they were appointed important cultural assets of Japan. In addition, along the River Nakajima, there are many other stone bridges like Momotani, Oide, Amigasa, Furumachi, Ichiran, Susukihara, Higashi-shin and Fukuro bridges, which rated as important cultural properties by the city and have formed the sights of the city.

This Nakajima River, running through the center of Nagasaki City, was struck by the aforementioned local downpour and the flooding took place which submerged the road surfaces of these stone bridges. Dynamic water pressure generated by the fast flood flow (3.5 m/sec to 4.0 m/sec) took away the arch spandrel and upper railings of the Momotani, Megane and Fukuro bridges, but left the arch stones. Six other bridges were completely destroyed and only some of the bridge foundations were left.

* Member of JSCE, Dr. Eng., Professor, Department of Civil Engineering, Nagasaki University
(Bunkyo-machi 1-14, Nagasaki City, Nagasaki 852, Japan)

Since these bridges provide the city's road network with arteries, they have been playing an important role in the city transportation, especially as escape ways for emergency or as access for the reconstruction works after a disaster.

On the other hand, when submerged by floodwater, the stone arch bridges tent to block 21 % to 54 % of the total stream area thus aggravating the flood and increasing the damage by the dumup effect[1]~[3].

To study the effect of the stone arch bridge on the flood flow and to measure the hydrodynamic pressure required to destroy, the stone bridge was tested by means of setting up a scaleddown model of the Fukuro bridge in the test water channel. The combined effects on the arch stones caused by drag, lift, yawing moment, pitching moment and rolling moment were measured through the experimentation of the model stone arch bridge. As a result of calculating the resistance of the stone arch bridge against flood flow, using the values obtained, we confirmed, that, as far as the Fukuro bridge is concerned, the arch stones were stable[4]~[6].

Collapse tests of the flood flow pressure on a stone arch bridge model of the same construction as the actual bridge were also carried out.

2. EXPERIMENTATION ON FULL MODEL OF THE ARCH BRIDGE

(1) Dimensions of Model Arch Bridge

Fig. 1 shows the scale of the full model of the Fukuro bridge. A 1/38.5 scaled model is used. The test water channel has the total length of 15.232 m, the width of 39.5 cm and the bed slope of $i=1/97.4$.
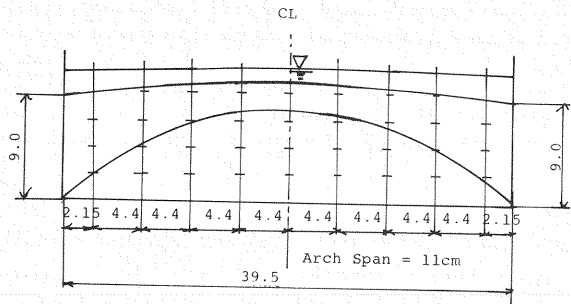

Fig. 1 Dimensions of Full Fukuro Bridge Model.

(2) Experimental Findings

a)   The average velocity, water depth and flow discharge of stream, when an arch bridge was not provided, are indicated in Table 1.

Table 1 Normal hydraulic quantity when not obstructed by arch bridge.

Position	Average velocity U (cm/sec)	Average water depth H (cm)	Flow discharge Q (m³/ sec)
10cm upstream	123.4	5.27	0.0257
At center	123.9	5.17	0.0253
10cm downstream	124.7	5.11	0.0252
Average			0.0254

b)   Table 2 shows the hydraulic quantity and the distribution of water depth and of velocity as well as their measured values, in the presence of a stone arch bridge.

From Table 2 we can see that the water depth of a stream with an arch bridge is 2.27 to 2.38 times higher upstream than without a bridge and 1.21 times higher even down stream. Fig. 2 indicates how water depth at the stream center changes before and after the existence of the arch bridge.

It will be noted that the water depth of a steep slope river flow rises suddenly and causes a dammed-up effect when an arch bridge is submerged by flood. The Froude rate F in this case is calculated as 1.57 and

Table 2　Hydraulic quantity when obstructed by arch bridge.

| Position	Average velocity U (cm / sec)	Average water depth H (cm)	Flow discharge Q (m³ / sec)	Rate of increase
300cm upstream	110.3	5.3	0.0231	
280cm upstream	110.0	5.2	0.0226	
200cm upstream	56.0	8.8	0.0196	
150cm upstream	64.5	9.8	0.0250	
100cm upatream	56.2	10.6	0.0235	
50cm upstream	52.9	11.5	0.0239	
25cm upstream	53.0	11.4	0.0238	
10cm upstream	51.5	11.7	0.0238	2.27
1cm upstream	46.4	12.3	0.0225	2.38
At center	76.6	10.2		1.98
1cm downstream	50.6	11.7	0.0233	2.26
10cm downstream	105.9	6.2	0.0259	1.21
25cm downstream	109.1	5.8	0.0250	
50cm downstream	111.2	5.3	0.0233	
110cm downstream	117.6	5.0	0.0234	
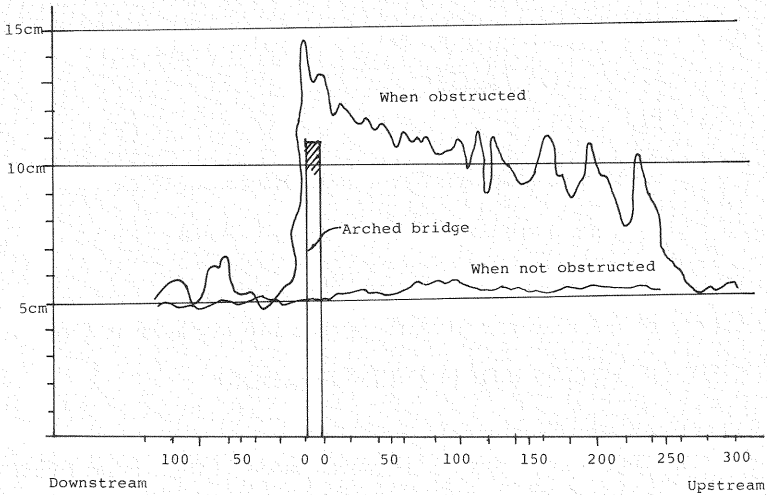
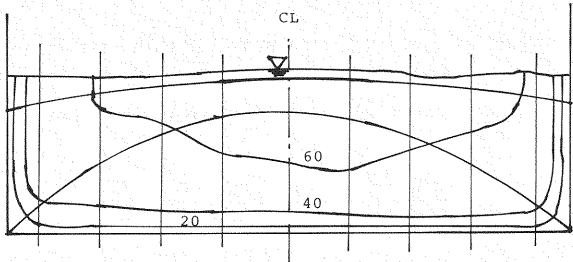**Fig. 2**　Water surface profile at center line of stream.

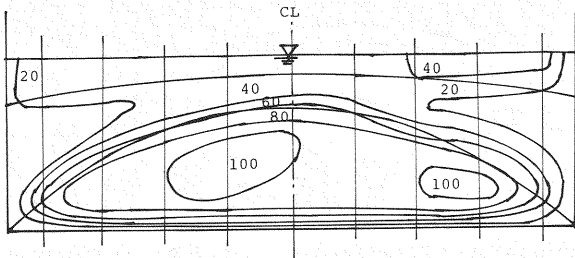**Fig. 3**　Distributions of velocity at 1 cm downstream.

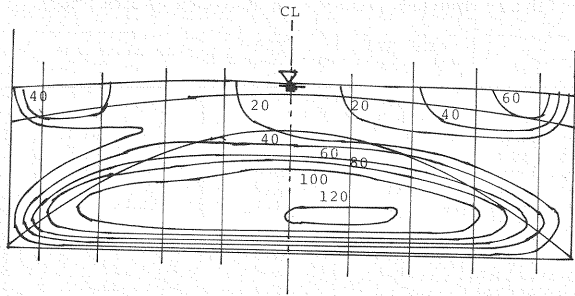**Fig. 4**　Distributions of velocity at 10 cm downstream.

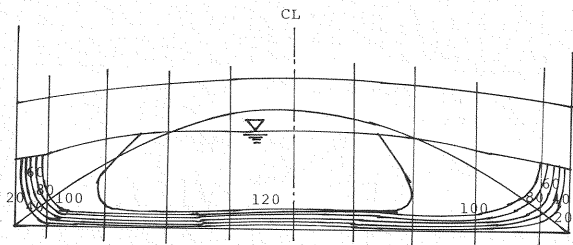Fig. 5 Distributions of velocity at 1 cm downstream.

Fig. 6 Distributions of velocity at 10 cm downstream.

the undular jump takes place as indicated in Fig. 2[7].

Sectional distributions of the velocity across the stream are as shown in Fig. 3 to 6.

3.   EXPERIMENT OF STONE ARCH BRIDGE MODEL

(1)   Model Dimensions and Experimental Facilities

The experiment was carried out by putting a 1/38.5 scale model of the existing Fukuro bridge into the test water channel with the width of 40 cm and the slope of 1/94.14 to reproduce the flood condition. Fig. 7 shows a beam instrument used for measuring load and Fig. 8 shows the construction of the model stone arch.

Load magnitudes on arch stones ②, ③······⑫ were measured with a strain meter by detecting strains on load converters tied by piano wires of 0.5 mmϕ to the lift measurement points ①, ②, ③ and ④ and the drag measurement points ⑤, ⑥, ⑦, and ⑧. An alienating paper is inserted in the 2 mm gap between arch
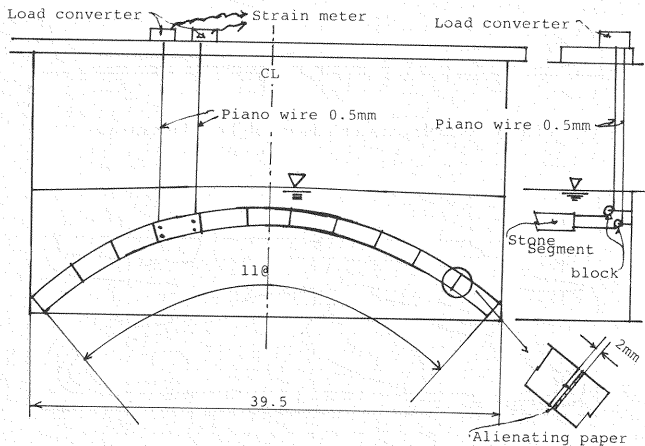

Fig. 7 Illustration of model experimental facilities.

Fig. 8 Fukuro bridge model.

stones as illustrated in Fig. 7 in order to plug water to avoid hydraulic stress and to lower frictional coefficient between the stones. The magnitudes and application points of resultant flow forces working on each arch stone were thus measured, and such external forces determining the limiting hydrodynamic fracture stress on the stone arch bridge as flow pressure, drag, lift (static water pressure+lift), horizontal pressure, yawing moment, rolling moment and pitching moment were computed from the measured values.

The resultant forces were measured about fifty times at the measuring points ①, ②, ③, ④, ⑤, ⑥, ⑦ and ⑧ for the eleven arch stones ② to ⑫. Histograms for No. 2-②, No. 7-② and No. 12-④ are given in Fig. 9(a), (b) and (c). F_m means the average measurement value (g) ; F_{max} means the maximum value (g), F_{min} the minimum (g) and σ is the standerd deviation. The measured values, in general, suggest that there are relatively large amounts of standard deviations of the lift of 2~6 (actually, lift+static water pressure), while that of the draft is rather limited to 0.3~1.0. For the three different kinds of stresses and the three kinds of moments affecting the resultant flood forces working on the arch stones, it is found from the measurement values at the points ①, ②, ③, ④, ⑤, ⑥, ⑦ and ⑧ that the lift+ static water pressure P_v(g), the drag P_h (g) and the moment SM_x (g-cm) are the governing factors in the case of stone arch bridges.

Fm=107.56-63.9=43.66
Fmax=122, Fmin=94
α=6.444

Fm=52.69-37.0=15.69
Fmax=70, Fmin=45
α=4.002

Fm=101.45-61.3=40.15
Fmax=114, Fmin=89
α=5.180

Fig. 9(a) Histogram of resultant forces at point lift ② working on Stone segment No. 2.

Fig. 9(b) Histogram of resultant forces at point lift ③ working on Stone segment No. 7.

Fig. 9(c) Histogram of resultant forces at point lift ④ working on Stone segment No. 12.

Table 3　Values of F_m.

Stone number	1	2	3	4	5	6	7	8
2	7.38	43.7	2.4	7.0	4.98	6.06	3.97	6.17
3	9.03	33.3	3.0	15.8	8.50	3.22	6.02	7.76
4	16.27	24.7	7.5	16.2	5.53	4.12	7.17	7.05
5	15.21	16.3	11.5	13.0	5.80	3.85	7.57	5.34
6	8.29	9.4	5.3	12.1	3.71	3.84	6.12	6.69
7	7.21	15.7	6.4	12.9	4.15	4.50	2.44	4.35
7A	4.58	13.3	6.0	13.8	1.16	1.29	1.49	2.79
8	4.89	18.2	9.3	16.2	3.54	3.11	4.32	4.35
9	9.84	11.5	14.3	17.0	5.44	8.60	4.62	6.62
10	6.50	17.4	21.0	22.5	4.22	8.16	4.86	8.10
11	0.80	9.1	13.7	37.2	2.42	4.10	11.54	8.64
12	4.59	9.1	8.9	40.2	6.32	4.58	6.00	5.33

Table 4　P_h, P_v and other parameters (symmetrically rearranged).

Stone number	Ph (g)	Pv (g)	SMx (g-cm)	Cd	Cl	Static water pressure (g)	U (cm/s)
2	21.7	61.6	180.6	1.14	2.01	214.2	85.8
3	26.1	61.0	160.4	1.21	1.15	166.9	90.9
4	24.6	66.0	69.2	1.12	0.59	124.4	87.7
5	23.9	54.4	16.4	0.73	0.23	88.6	106.5
6	17.8	41.9	62.8	0.51	0.16	66.4	111.1
7	11.0	40.0	76.6	0.25	0.13	61.0	111.7

　　Table 3 shows the average values of F_m at the measuring points of each arch stone. In Table 4, the drag P_h (g), the lift + static water pressure P_v(g), the pitching moment SM_x (g-cm), the drag coefficient C_d, the lift coefficient C_1 and the static water pressure P_s (g), and the average flow speed at 90 cm of the upper stream U (cm/sec), are given as calculated values out of the three kinds of stresses and the three kinds of moments mentioned above. The values of P_v, P_h and pitching moment SM_x obtained from Table 4 are shown in Fig. 10. Although the actual measurement values in Table 3, Table 4 and Fig. 10 are in fact not necessarily symmetrical, these were averaged for the purpose of structual calculation.

　　Larger values of P_v are distributed around one quarter from the supports, while those become smaller at the middle point and at the both ends. The drag P_h and P_v have a similar tendency. However, SM_x becomes substantially larger near the bridge supports, smallest around the point 5 and slightly larger again at the middle stone. If the drag coefficient C_d and the lift coefficient C_1 are calculated by Equations (1) and (2), the results are as shown in Fig. 11, indicating smaller values in the center.

$$C_d = \frac{P_h}{1/2\,\rho\,U^2 \times A} \text{ for } A = B \times T \quad\cdots\cdots\cdots\cdots\cdots\cdots\cdots\cdots\cdots\cdots\cdots\cdots\cdots\cdots\cdots\cdots\cdots\cdots\cdots (1)$$

$$C_1 = \frac{P_v - P_s}{1/2\,\rho\,U^2 \times A'} \text{ for } A' = B' \times L \cdots\cdots\cdots\cdots\cdots\cdots\cdots\cdots\cdots\cdots\cdots\cdots\cdots\cdots\cdots\cdots (2)$$

where,　　ρ : density of water
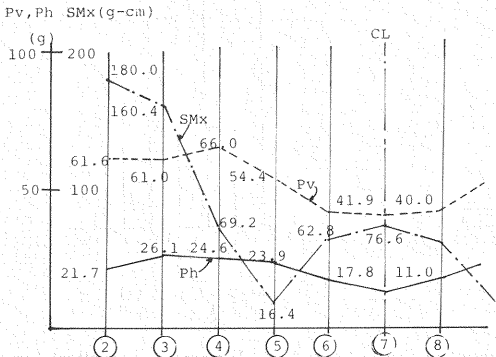
　　　　　B : width of stone segment

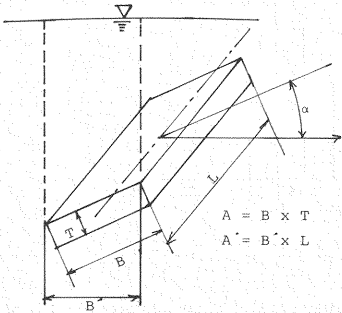Fig. 10　Drag P_h, lift (+static water pressure) P_v and pitching moment M_x caused by flood flow.
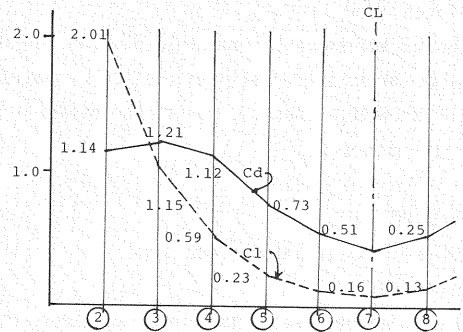

Fig. 11　Picture of A and A'.

Fig. 12 Drag coefficient C_d and lift coefficie C_l.

B' : projected width of stone segment on horizontal axis

T : height of stone segment

L : length of stone segment

4. STABILITY OF STONE ARCH BRIDGES AGAINST FLOOD FLOW

(1) Experimental Results and Structural Analysis

A three-dimensional construction illustrated in **Fig. 8** was studied for structural analysis using the measurement values of the drag P_h (g), the lift+static water pressure P_v (g) and the pitching moment SM_x (g-cm).

For the purpose of the structural analysis, Solid Finite Element Structural Analysis Program referred to in Reference 8) was used. Elastic coefficients of the stone segment used for the model arch bridge were measured as follows :

$E=5.76 \times 10^4$ kg/cm^2,

Poisson's ratio $\nu=0.18$,

$G=2.43 \times 10^4$ kg/cm^2.

The weight of each stone segment is 2.23 g/cm^3 and the underwater coefficient of friction between arch stones is $\mu=0.67$. Through the structural analysis it was observed that the axial force F_x (g), the shearing stress F_z (g) and the flexural moment M_y (g-cm) due to the in-plane arch action, and the shering stress F_y (g), the torque T (g-cm) and the flexural moment M_z (g-cm) due to the out-of-plane arch action, occurred as indicated in **Table 5**.

Table 5 Three-dimensional on arch bridge.

Number of panel point	Axial load F_x (g)	Shearing stress (out-of-plane) F_y (g)	Shearing stress (in-plane) F_z (g)	Torque SM_x (g-cm)	Flexure in-plane SM_y (g-cm)	Flexure out-of-plane SM_z (g-cm)
1	-897.3	119.7	4.2	-163.7	-102.7	-218.2
3	-832.8	98.0	40.5	-25.4	-130.3	115.1
5	-778.1	71.9	50.3	74.0	-54.1	366.7
7	-735.2	47.3	37.6	73.2	23.1	564.4
9	-710.2	23.4	27.4	7.9	61.2	686.4
11	-699.3	5.5	23.5	-16.4	76.7	728.4
13	-699.4	-5.5	18.3	-27.0	76.7	728.4

(2) Calculation of Stability of Stone Arch Bridges against Hydrodynamic Pressures

Shearing stress, τ_1, generated by torque is ;

$$\tau_1 = T/J \cdot t \quad\quad\quad\quad\quad\quad\quad\quad\quad\quad\quad\quad (3)$$

where, T : torque

J : torsional resistance, $J=1/3\ b t^3$

b : span of arch stones (cm)

t : height of arch stones (cm)

Bridge stability against the shearing stress can be maintained by frictional stress due to the arch thrust.

Such a frictional stress due to the arch thrust also provides stability against the shearing stress τ_2 due to the in-plane arch action and the shearing stress τ_3 due to the out-of-plane arch action. The allowable shearing stress τ_a due to the friction is;

$$\tau_a = Fx / A \times u \quad\cdots\cdots\cdots (4)$$

where, F_x : axial force of arch rib (g),

A : cross-sectional area of frictional surface (cm^2),

μ : friction coefficient$=0.67$.

The area A which is subjected to moment and axial force, as illustrated in **Fig. 13**, is odtained by the following equations :

$$\left.\begin{array}{l} M = Pe \\ N = P \end{array}\right\} \quad\cdots\cdots\cdots (5)$$

$$\left.\begin{array}{l} \sigma_1 = \sigma_N + \sigma_B = P/B(1+6\,e/B) \\ \sigma_2 = \sigma_N - \sigma_B = P/B(1-6\,e/B) \end{array}\right\} \quad\cdots\cdots\cdots (6)$$

$$B_1 = B^2(1+6\,e/B)/12\,e \quad\cdots\cdots\cdots (7)$$

$$A = B_1 \cdot T \quad\cdots\cdots\cdots (8)$$

where, B : interval of arch stones (cm)

e : eccentric distance of application point of resultant force P (cm)

σ_1, σ_2 : resultant stresses due to moment M and axial force N

T : height of arch stones (cm)

B_1 : width of frictional surface (cm)

When the resultant stress of τ_1, τ_2 and τ_3 becomes larger than τ_a due to the increased flow speed, then the stability of sealing matrial between arch stones is lost so that they may start rotating or slipping, and finally the bridge will collapse. **Fig. 14** shows the calculated results, proving that the stability was maintained in the model arch.
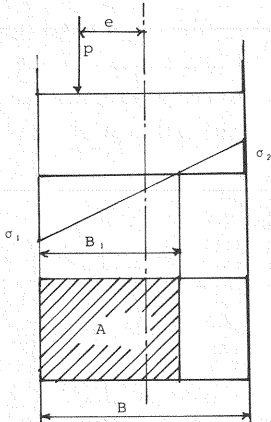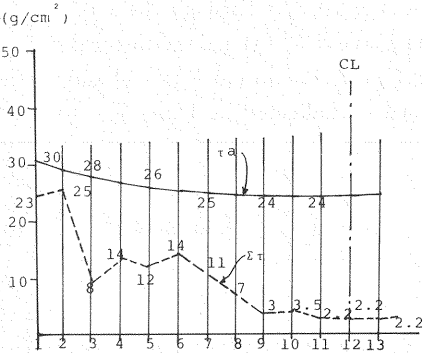

Fig. 13   Frictional surface area A.

Fig. 14   Results of Stability calculation with experimental values.

5.   COLLAPSE TEST OF MODEL STONE ARCH BRIDGE

For the collapse test under fllod flow a model stone arch bridge using the same number of stones as the existing bridge and scaled down to 1/38.5, was installed in the experimental water channel with the 1/94.14 flow slope. The process of collape was filmed on a video camera. From **Photo 1**, **Photo 2** and **Photo 3**, the following stages of damage and collapse produced in the experiment can be observed. The road
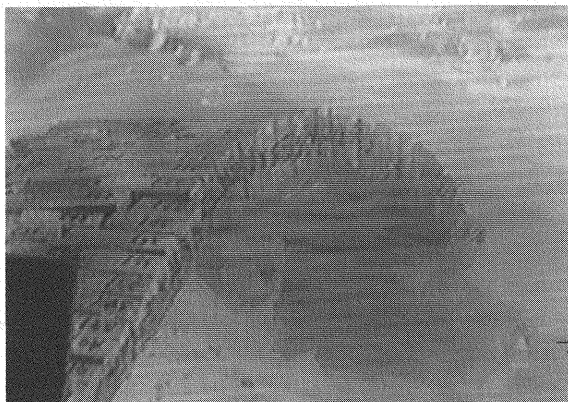
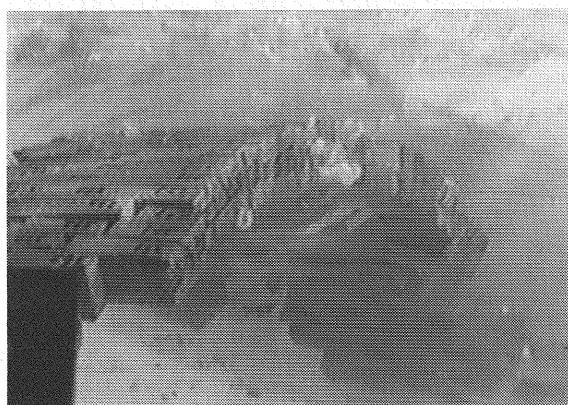Photo 1   Collapse of arch stones (1).
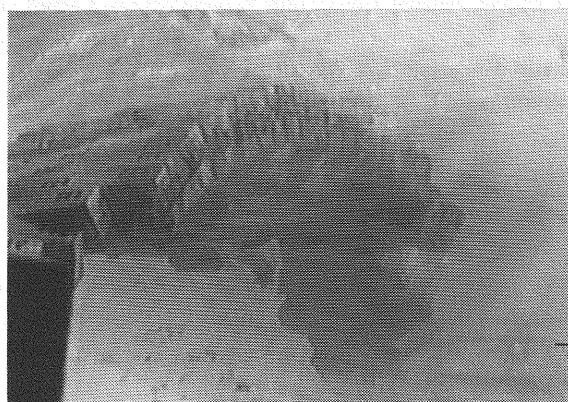

Photo 2   Collapse of arch stones (2).

Photo 3   Collapse of arch stones (3).

surface and spandrel of the arch bridge were washed away soon after the bridge was submerged, but the arch stones did not collapse. However, after being flooded for a long time, the seal started gradually to slip out and the arch stones to move. Finally, the sealant gap became larger and then the bridge collapsed. The details are shown in Photos 1~3.

The flow velocity which actually acted on the bridge when flooded can be assumed from the results of the

experiment as follows :

$$\left(\frac{U_m}{U_p}\right)^2 = \frac{h_m}{h_p} = \frac{1}{S} = \frac{1}{38.5} \quad\text{..}\quad (9)$$

where, U_p : actual flow speed of flood
  U_m : experimental flow speed
  h_m : experimental water level
  h_p : actual water level in flood
  S : scale of model to actual bridge.

If we apply U_m=99. 6 cm/sec and S=38. 5, then the assumed actual velocity speed becomes $U_p = U_m \times$ $\sqrt{38.5}$ =99. 6×$\sqrt{38.5}$=6. 2 m/sec. This means that the extraordinarily rapid flood flow of 6. 2 m/sec is needed to actually destroy the bridge. Assuming that the bridge can start to collapse if submerged for a long time in the flow of 1 m/sec, the limit velocity speed for the Fukuro bridge is calculated about 6. 2 m/sec. This assumption is borne out by the fact that in the Nagasaki flood the estimated flow speed was 3. 5 to 4. 0 m/sec and that the arch stones of the Fukuro bridge remained safe although the spandrel parts were lost.

6. CONCLUSIONS

This experiment was intended for studying the influence of fllod flow on stone arch bridges and their hydrodynamic stability by means of making a model bridge on 1/38. 5 scale and reproducing a flood condition by running water of 0. 0235 m³/sec in an experimental waterway.

The following conclusions were obtained.

(1) The experimental flow discharge is calculated to be 216 m³/sec for the actual bridge and this corrsponds to 68 % of the flow of 320 m³/sec estimated for the flood.

(2) It was recorded in the experiment using the full bridge model that water level upstream rises by the ratio of 2. 27 to 2. 38 when the flow was blocked by the arch bridge. This fact underlines possible danger of flood, aggrevated by a damming-up effect due to the bridge obstacle, particularly in steep slope rivers.

(3) In this case the Froude number F was 1. 57 and undular jump was observed.

(4) In the test to measure the resultant hydrodynamic forces acting on the arch stones by putting a model stone arch bridge in a reproduced flood flow, a substantial amount of standard deveation was recorded due to the jet stream and due to the existence of cavitation down-stream the arch stones.

(5) Due to the hydrodynamic forces mentioned above, when the shearing stress caused by torque due to the out-of-plane arch action, the shearing stress due to the in-plane arch action and the shearing stress due to the out-of-plane arch action, exceed the frictional resistance prodeced by the axial torque of the arch sealing, the sealing between the arch stones loses stability so that they start rotating or slipping and finally the collapse will take place. In the experiment, however, such a collapse may not have occurred and the arch stones stayed safe.

(6) The arch spandrel of the model stone arch bridge using the same number of stones as the actual bridge was immediately carried away in the collapse test, though the stone segments were not destroyed. However, when left in the flow for a long time, the sealant slipped away, the stone segments also dropped off and the bridge collapsed.

In this study the author was able to carry out a structural analysis to explain the collapse mechanism in a stone arch bridge as a solid structure. Further experiments and structural analyses to get more precise knowledge of the collapse mechanism in solid stone structures are planned in the future.

ACKNOWLEDGEMENTS

continuously in progress for Megane Bridge.

REFERENCES

1) The Technical Mission of Nagasaki University led by Y. Konishi : "Report on Flood Disaster in Nagasaki Experienced in July 1982——Bridges", pp. 79~90, 1982.

2) Konishi, Y. : "An Report on Flood Disaster in July 1982——Damage to Bridgs", A Study Report on National Disasters subsidized by the Scientific Research Fund of the Ministry of Education (No. 57020201), pp. 109~116, 1983.

3) Konishi, Y. : On Damages to Stone Arch Bridges by Flood, Preprint of Annual Conference of Western Branch of the Japan Society of Civil Engineers, pp. 90~91, 1983.

4) Konishi, Y., Takemasa, T. and Nagata, M. : An Experimental Study on the Hydrodynamic. Influences of the Stone Arch Bridge on Flood Flow, Preprint of Annual Conference of Western Branch of the Japan Society of Civil Engineers, pp. 42~43, 1984.

5) Konishi, Y., Takemasa, T. and Nagata, M. : An Experimental Study on the Hydrodynamic Influences of the Stone Arch Bridge on Flood Flow (2 nd Report), Preprint of Annual Conference of Western Branch of the Japan Society of Civil Engineers, pp. 46~47, 1985.

6) Konichi, Y., Takemasa, T. and Nagata, M. : An Experimental Study on the Hydrodynamic Influences of the Stone Arch Bridge on Flood Flow (3 rd Report), Preprint of Western Branch of the Japan Society of Civil Engineers, pp. 10~11, 1986.

7) Murota, A. : Applied Hydrodynamics, Kyoritsu Shuppan, Tokyo, 1969.

8) Kobori, T. and Yoshida, H. : The Structural Analysis Program by Finite Element Method, Maruzen, Tokyo, pp. 62~73, 1980.